Inorg. Chem. **2003**, *42*, 2094–2101

Remarkable Dynamical Opening and Closing of Platinum and Palladium Pentaruthenium Carbido Carbonyl Cluster Complexes

Richard D. Adams,* Burjor Captain, Wei Fu, Perry J. Pellechia, and Mark D. Smith

Department of Chemistry and Biochemistry and the USC Nanocenter, University of South Carolina, Columbia, South Carolina 29208

Received November 4, 2002

The reaction of $Ru_5(CO)_{15}(\mu_5\text{-C})$, **1**, with $Pt(PBu^t_3)_2$ at room temperature yielded the mixed-metal cluster complex $PtRu_5(CO)_{15}(PBu^t_3)(C)$, **2**, in 52% yield. Compound **2** consists of a mixture of two interconverting isomers in solution. One isomer, **2A**, can be isolated by crystallization from benzene/octane solvent. The second isomer, **2B**, can be isolated by crystallization from diethyl ether. Both were characterized crystallographically. Isomer **2A** consists of a square pyramidal cluster of five ruthenium atoms with a phosphine-substituted platinum atom spanning the square base. Isomer **2B** consists of a square pyramidal cluster of five ruthenium atoms with a phosphine-substituted platinum atom on an edge on the square base. The two isomers interconvert rapidly on the NMR time scale at 40 °C, $\Delta G_{313}^{\ddagger} = 11.4(8)$ kcal mol^{-1}, $\Delta H^{\ddagger} = 8.8(5)$ kcal mol^{-1}, $\Delta S^{\ddagger} = -8.4(9)$ cal mol^{-1} K^{-1}. The reaction of $Pd(PBu^t_3)_2$ with compound **1** yielded two new cluster complexes: $PdRu_5(CO)_{15}(PBu^t_3)(\mu_6\text{-C})$, **3**, in 50% yield and $Pd_2Ru_5(CO)_{15}(PBu^t_3)_2(\mu_6\text{-C})$, **4**, in 6% yield. The yield of **4** was increased to 47% when an excess of $Pd(PBu^t_3)_2$ was used. In the solid state compound **3** is structurally analogous to **2A**, but in solution it also exists as a mixture of interconverting isomers; $\Delta G_{298}^{\ddagger} = 10.6(6)$ kcal mol^{-1}, $\Delta H^{\ddagger} = 9.7(3)$ kcal mol^{-1}, and $\Delta S^{\ddagger} = -3(1)$ cal mol^{-1} K^{-1} for **3**. Compound **4** contains an octahedral cluster consisting of one palladium atom and five ruthenium atoms with an interstitial carbido ligand in the center of the octahedron, but it also has one additional $Pd(PBu^t_3)$ grouping that is capping a triangular face of the ruthenium cluster. The $Pd(PBu^t_3)$ groups in **4** also undergo dynamical interchange that is rapid on the NMR time scale at 25 °C; $\Delta G_{298}^{\ddagger} = 11(1)$ kcal mol^{-1}, $\Delta H^{\ddagger} = 10.2(4)$ kcal mol^{-1}, and $\Delta S^{\ddagger} = -3(2)$ cal mol^{-1} K^{-1} for **4**.

Introduction

Mixed-metal heterogeneous catalysts have attracted much interest because of their superior catalytic properties.[1] It has been suggested that the presence of different metals in the proximity of a catalytically active site leads to a higher reactivity in certain cases.[2] It has been proposed that a metal atom can activate its neighbor simply by donation of electron density.[3]

Mixed-metal cluster complexes have been shown to be good precursors to supported bimetallic nanoparticles[4−11] and supported heterogeneous catalysts.[12] Palladium−ruthenium and platinum−ruthenium clusters supported on mesoporous silica have been shown to exhibit high catalytic activity for certain hydrogenation reactions.[12] Platinum−ruthenium cata-

* Author to whom correspondence should be addressed. E-mail: adams@mail.chem.sc.edu.

(1) (a) Sinfelt, J. H. *Bimetallic Catalysts: Discoveries, Concepts and Applications*; Wiley: New York, 1983. (b) Sinfelt, J. H. Bifunctional Catalysis. *Adv. Chem. Eng.* **1964**, *5*, 37. (c) Sinfelt, J. H. *Sci. Am.* **2985**, *253*, 90.
(2) (a) Goodman, D. W.; Houston, J. E. *Science* **1987**, *236*, 403. (b) Ichikawa, M. *Adv. Catal.* **1992**, *38*, 283.
(3) (a) Adams, R. D.; Barnard, T. S. *Organometallics* **1998**, *17*, 2885. (b) Sachtler, W. M. H. *Faraday Discuss. Chem. Soc.* **1981**, *72*, 7. (c) Sachtler, W. M. H. *J. Mol. Catal.* **1984**, *25*, 1. (d) Guczi, L. *J. Mol. Catal.* **1984**, *25*, 13. (e) Sachtler, W. M. H.; van Santen, R. A. *Adv. Catal.* **1977**, *26*, 69.
(4) Toshima, N.; Yonezawa, T. *New J. Chem.* **1998**, 1179.
(5) Johnson, B. F. G. *Coord. Chem. Rev.* **1999**, *192*, 1269.
(6) Midgley, P. A.; Weyland, M.; Thomas, J. M.; Johnson, B. F. G. *Chem. Commun.* **2001**, 907.
(7) Nashner, M. S.; Frenkel, A. I.; Somerville, D.; Hills, C. W.; Shapley, J. R.; Nuzzo, R. G. *J. Am. Chem. Soc.* **1998**, *120*, 8093.
(8) Nashner, M. S.; Frenkel, A. I.; Adler, D. L.; Shapley, J. R.; Nuzzo, R. G. *J. Am. Chem. Soc.* **1997**, *119*, 7760.
(9) Shephard, D. S.; Maschmeyer, T.; Johnson, B. F. G.; Thomas, J. M.; Sankar, G.; Ozkaya, D.; Zhou, W.; Oldroyd, R. D.; Bell, R. G. *Angew. Chem., Int. Ed. Engl.* **1997**, *36*, 2242.
(10) Raja, R.; Sankar, G.; Hermans, S.; Shephard, D. S.; Bromley, S.; Thomas, J. M.; Johnson, B. F. G. *Chem. Commun.* **1999**, 1571.
(11) Shephard, D. S.; Maschmeyer, T.; Sankar, G.; Thomas, J. M.; Ozkaya, D.; Johnson, B. F. G.; Raja, R.; Oldroyd, R. D.; Bell, R. G. *Chem.—Eur. J.* **1998**, *4*, 1214.

10.1021/ic020656o CCC: $25.00
Published on Web 02/21/2003

lysts are the most effective catalysts for the oxidation of methanol at the anode of the direct methanol fuel cell.[13]

There has been much interest in molecular dynamics of metal clusters, but most of these studies have been focused on the dynamical rearrangements of the ligand structures;[14] however, there have been some interesting examples of cluster isomerism with dynamical interconversions.[15]

We have recently found that $Pd(PBu^t_3)_2$ reacts with ruthenium carbonyl cluster complexes by addition of $Pd(PBu^t_3)$ groups to the metal−metal bonds.[16] Here we report on the reaction of $Ru_5(CO)_{15}(\mu_5\text{-C})$,[17] **1**, with $Pt(PBu^t_3)_2$ and $Pd(PBu^t_3)_2$. The reaction of **1** with $Pt(PBu^t_3)_2$ yielded the adduct $PtRu_5(CO)_{15}(PBu^t_3)(C)$, **2**, that exists in solution as two isomers that interconvert rapidly on the NMR time scale by a process that resembles the diffusion of metal adatoms across a metal surface.[18] The reaction of **1** with $Pd(PBu^t_3)_2$ yielded the new ruthenium−palladium adducts $Pd_nRu_5(CO)_{15}(PBu^t_3)_n(\mu_6\text{-C})$, where $n = 1$ (compound **3)** or 2 (compound **4**). A preliminary report of our studies of **2** has been published.[18]

Experimental Section

General Data. Infrared spectra were recorded on a Nicolet 5DXBO FTIR spectrophotometer. ^{1}H NMR and ^{31}P NMR spectra were recorded on a Varian Inova 500 spectrometer operating at 500.22 and 202.52 MHz, respectively. All NMR measurements were made in methylene chloride-d_2 solvent. ^{31}P NMR spectra (externally referenced against 85% ortho-H_3PO_4). Elemental analyses were performed by Desert Analytics (Tucson, AZ). Bis(tri-*tert*-butylphosphine)palladium(0), $Pd(PBu^t_3)_2$, was purchased from Strem and was used without further purification. $Ru_5(CO)_{15}(\mu_5\text{-C})$, **1**,[17] and bis(tri-*tert*-butylphosphine)palladium(0), $Pt(PBu^t_3)_2$,[19] were prepared according to published procedures. Product separations were performed by TLC in air on Analtech 0.25 and 0.5 mm silica gel 60 Å F_{254} glass plates.

Synthesis of $Ru_5Pt(CO)_{15}(PBu^t_3)(C)$, 2. An 18.0 mg sample of **1** (0.019 mmol) was allowed to react with 10.5 mg of $Pt(PBu^t_3)_2$ (0.017 mmol) in 15 mL of freshly distilled CH_2Cl_2 under a nitrogen atmosphere at room temperature for 30 min. The solvent was removed in vacuo, and the product was isolated by TLC by using hexane solvent to yield 13.2 mg (52%) of red **2**: IR ν_{CO} (cm^{-1}; in CH_2Cl_2): 2087 (m), 2055 (s), 2033 (s), 2028 (s), 1991 (sh), 1822 (w, br). ^{31}P{^{1}H} NMR at −40 °C (in d_8-toluene): $\delta = 118.2$ ppm ($^1J_{Pt-P} = 5983$ Hz), $\delta = 92.7$ ppm ($^1J_{Pt-P} = 6164$ Hz). Anal. Calcd: C, 25.19; H, 2.02. Found: C, 25.28; H, 1.92.

Synthesis of $Ru_5Pd(CO)_{15}(PBu^t_3)(\mu_6\text{-C})$, 3, and $Ru_5Pd_2(CO)_{15}(PBu^t_3)_2(\mu_6\text{-C})$, 4. A 20.2 mg sample of **1** (0.022 mmol) was dissolved in 15 mL of freshly distilled CH_2Cl_2 in a 25 mL three-neck round-bottom flask, 9.2 mg of $Pd(PBu^t_3)_2$ (0.018 mmol) was added, and the reaction mixture was then stirred at room temperature for 30 min. The solvent was removed in vacuo, and the products were separated by TLC by using hexane as the elution solvent to yield 13.4 mg (50%) of **3** and 2.0 mg (6%) of **4**. Spectral data for **3**: IR ν_{CO} (cm^{-1}; in CH_2Cl_2): 2087 (m), 2055 (vs), 2037 (s), 2027 (s), 1991 (sh), 1860 (w, br). ^{1}H NMR (CD_2Cl_2 at −90 °C): $\delta =$ 1.43 ppm (d, 9H, CH_3, $^3J_{P-H} = 6.6$ Hz), $\delta = 1.29$ ppm (d, 18H, CH_3, $^3J_{P-H} = 14.9$ Hz). ^{31}P{^{1}H} NMR (CD_2Cl_2 at −75 °C): $\delta =$ 86.76 ppm (major isomer **3A**, 80%), $\delta = 83.32$ ppm (minor isomer **3B**, 20%). Anal. Calcd: C, 26.97; H, 2.17. Found: C, 26.66; H, 2.09. Spectral data for **4**: IR ν_{CO} (cm^{-1}; in CH_2Cl_2): 2071 (m), 2036 (vs), 2009 (s), 1978 (sh), 1852 (w, br), 1814 (w, br). ^{1}H NMR (CD_2Cl_2 at −90 °C): $\delta = 1.44$ ppm (d, 9H, CH_3, $^3J_{P-H} = 6.4$ Hz), $\delta = 1.40$ ppm (d, 9H, CH_3, $^3J_{P-H} = 6.8$ Hz), $\delta = 1.32$ ppm (d, 18H, CH_3, $^3J_{P-H} = 14.9$ Hz). $\delta = 1.24$ ppm (d, 18H, CH_3, $^3J_{P-H} = 14.7$ Hz). ^{31}P{^{1}H} NMR (CD_2Cl_2 at −65 °C): $\delta = 82.20$ ppm (s, 1P), $\delta = 81.40$ ppm (s, 1P). Anal. Calcd: C, 30.88; H, 3.47. Found: C, 31.02; H, 3.34.

Improved Yield of 4. An 11.4 mg amount of **1** (0.012 mmol) was dissolved in 35 mL of freshly distilled CH_2Cl_2 in a 50 mL three-neck round-bottom flask, to which 29.7 mg of $Pd(PBu^t_3)_2$ (0.058 mmol) was added, and the reaction mixture was then stirred at room temperature for 30 min. The product was separated by TLC by using hexane to yield 8.9 mg (47%) of **4**.

NMR Calculations. Line shape analyses were performed on a Gateway PC by using the program EXCHANGE written by R. E. D. McClung of the Department of Chemistry, University of Alberta, Edmonton, Alberta, Canada. For compound **2** exchange rates were determined at 13 different temperatures in the temperature range −40 to +60 °C. The activation parameters were determined from a best fit Eyring plot using the program Microsoft Excel 97: $\Delta H^{\ddagger} = 8.8(5)$ kcal mol^{-1}, $\Delta S^{\ddagger} = -8.4$ cal mol^{-1} K^{-1}. The thermodynamic parameters were derived from a ln K vs $1/T$ plot of the equilibrium constant K determined at seven different temperatures in the range −70 to −30 °C: $\Delta H° = -1.4(1)$ kcal mol^{-1}, $\Delta S° = -6.1(3)$ cal mol^{-1} K^{-1}. For compound **3**, exchange rates from the ^{1}H NMR spectra for the carbon−phosphorus bond rotation in tri-*tert*-butylphosphine were determined at five different temperatures in the temperature range −70 to −30 °C. The activation parameters were determined from a least-squares fit of an Eyring plot (ln[hk/K_BT] vs $1/T$) using the program Microsoft Excel 97: $\Delta H^{\ddagger} = 8.7(3)$ kcal mol^{-1}, $\Delta S^{\ddagger} = -7(2)$ cal mol^{-1} K^{-1}. Also exchange rates from ^{31}P NMR spectra for the $PdPBu^t_3$ group were determined at six different temperatures in the temperature range −75 to +25 °C. The activation parameters were determined from a least-squares fit of an Eyring plot (ln[hk/K_BT] vs $1/T$) using the program Microsoft Excel 97: $\Delta H^{\ddagger} = 9.7(3)$ kcal mol^{-1}, $\Delta S^{\ddagger} = -3(1)$ cal mol^{-1} K^{-1}. For compound **4**, exchange rates from ^{31}P NMR spectra for the two $PdPBu^t_3$ groups were determined at 11 different temperatures in the temperature range −65 to +25 °C. The activation parameters were determined from a least-squares fit of

(12) (a) Raja, R.; Khimyak, T.; Thomas, J. M.; Hermans, S.; Johnson, B. F. G. *Angew. Chem., Int.Ed.* **2001**, *40*, 4638. (b) Hermans, S.; Raja, R.; Thomas, J. M.; Johnson, B. F. G.; Sankar, G.; Gleeson, D. *Angew. Chem., Int. Ed.* **2001**, *40*, 1211. (c) Raja, R.; Sankar, G.; Hermans, S.; Shephard, D. S.; Bromley, S.; Thomas, J. M.; Johnson, B. F. G.; Maschemeyer, T. *Chem. Commun.* **1999**, 1571.

(13) (a) Tess, M. E.; Hill, P. L.; Torraca, K. E.; Kerr, M. E.; Abboud, K. A.; McElwee-White, L. *Inorg. Chem.* **2000**, *39*, 3942. (b) Schmidt, T. J.; Gasteiger, H. A.; Behm, R. J. *Electrochem. Commun.* **1999**, *1*, 1. (c) Hogarth, M. P.; Hards, G. A. *Platinum Met. Rev.* **1996**, *40*, 150. (d) Morimoto, Y.; Yeager, E. B. *Electroanal. Chem.* **1998**, *444*, 95.

(14) Farrugia, L. J.; Orpen, A. G. In *Metal Clusters in Chemistry*; Braunstein, P., Oro, L. A., Raithby, P. R., Eds.; Wiley-VCH: Weinheim, Germany, 1999; Vol. 2, p 1001.

(15) (a) Salter, I. D. In *Metal Clusters in Chemistry*; Braunstein, P., Oro, L. A., Raithby, P. R., Eds.; Wiley-VCH: Weinheim, Germany, 1999; Vol. 1, p 509. (b) Dyson, P. J. In *Metal Clusters in Chemistry*; Braunstein, P., Oro, L. A., Raithby, P. R., Eds.; Wiley-VCH: Weinheim, Germany, 1999; Vol. 2, p 1028.

(16) Adams, R. D.; Captain, B.; Fu, W.; Smith, M. D. *J. Am. Chem. Soc.* **2002**, *124*, 5628.

(17) Nicholls, J. N.; Vargas, M. D.; Hriljac, J.; Sailor, M. *Inorg. Synth.* **1989**, *26*, 283.

(18) Adams, R. D.; Captain, B.; Fu, W.; Pellechia, P. J.; Smith, M. D. *Angew. Chem., Int. Ed.* **2002**, *41*, 1951.

(19) Otsuka, S.; Yoshida, T.; Matsumoto, M.; Nakatsu, K. *J. Am. Chem. Soc.* **1976**, *98*, 5850.

Table 1. Crystallographic Data for Compound **2**

	2A		**2B**
empirical formula	$PtRu_5PO_{15}C_{28}H_{27}$		$PtRu_5PO_{15}C_{28}H_{27}$
fw	1334.91	1334.91	1334.91
cryst syst	triclinic	monoclinic	monoclinic
lattice params			
a (Å)	9.9510 (5)	12.4684 (10)	14.1957 (12)
b (Å)	12.1523 (6)	17.9669 (15)	18.0213 (15)
c (Å)	16.8957 (8)	17.3482 (14)	29.027 (2)
α (deg)	79.797 (1)	90	90
β (deg)	87.338 (1)	107.613(2)	92.113 (2)
γ (deg)	72.938 (1)	90	90
V (Å^3)	1922.31 (16)	3704.1 (5)	7420.9 (11)
space group	$P\bar{1}$	$P2_1/n$	$P2_1/c$
Z	2	4	8
ρ_{calcd} (g/cm^3)	2.31	2.39	2.39
μ(Mo Kα) (mm^{-1})	5.64	5.86	5.85
temp (K)	293	190	190
$2\theta_{max}$ (deg)	56.6	50.1	56.6
no. of obsd reflns ($I > 2\sigma(I)$)	7697	5594	14877
no. of params	460	458	919
GOF[a]	1.058	1.105	1.039
max shift in cycle	0.003	0.001	0.003
residuals: R1, wR2[a]	0.0384, 0.0941	0.0463, 0.0996	0.0379, 0.0764
abs correctn, max/min	SADABS, 1.00/0.69	SADABS, 0.831/0.616	SADABS, 0.583/0.389
largest peak in final diff map (e$^-$/Å^3)	1.569	2.397	1.745

[a] $R1 = \sum_{hkl}(||F_o| - |F_c||)/\sum_{hkl}|F_{obs}|$; $wR2 = [\sum_{hkl}w(|F_o| - |F_c|)^2/\sum_{hkl}wF_o^2]^{1/2}$, $w = 1/\sigma^2(F_o)$; $GOF = [\sum_{hkl}w(|F_o| - |F_c|)^2/(n_{data} - n_{vari})]^{1/2}$.

an Eyring plot ($\ln[hk/K_BT]$ vs $1/T$) using the program Microsoft Excel 97: $\Delta H^{\ddagger} = 10.2(4)$ kcal mol^{-1}, $\Delta S^{\ddagger} = -3(2)$ cal mol^{-1} K^{-1}.

Crystallographic Analysis. Dark red single crystals of isomer **2A** (triclinic and monoclinic forms) suitable for diffraction analysis were grown by slow evaporation of solvent from a benzene/octane solvent mixture at 5 °C. Dark red single crystals of isomer **2B** were obtained by slow evaporation of solvent from a diethyl ether solution at −25 °C. Dark red single crystals of **3** and **4** suitable for diffraction analysis were grown by slow evaporation of solvent from a hexane/methylene chloride solution at 5 °C and from a benzene/octane solution at room temperature, respectively. The data crystal for **2A** (triclinic) was glued onto the end of a thin glass fiber; all the others were frozen with inert oil onto fibers at 190 K. X-ray intensity data were measured using a Bruker SMART APEX CCD-based diffractometer using Mo Kα radiation ($\lambda = 0.71073$ Å). The raw data frames were integrated with SAINT+.[20] Corrections for Lorentz and polarization effects were also applied by using the program SAINT. An empirical absorption correction based on the multiple measurement of equivalent reflections was applied by using the program SADABS. All structures were solved by a combination of direct methods and difference Fourier syntheses, and refined by full-matrix least-squares on F^2, using the SHELXTL software package.[21] Crystal data, data collection parameters, and results of the analyses for the two isomers of compound **2** are listed in Table 1, and those for compounds **3** and **4** are listed in Table 2.

Table 2. Crystallographic Data for Compounds **3** and **4**

	3	**4**
empirical formula	$PdRu_5PO_{15}C_{28}H_{27}$	$Pd_2Ru_5P_2O_{15}C_{40}H_{54}$
fw	1246.22	1554.92
cryst syst	monoclinic	monoclinic
lattice params		
a (Å)	13.2248 (8)	20.1791 (15)
b (Å)	17.8173 (11)	15.2830 (11)
c (Å)	16.8949 (11)	17.9267 (13)
α (deg)	90	90
β (deg)	110.352(1)	114.165 (1)
γ (deg)	90	90
V (Å^3)	3732.4 (4)	5044.1 (6)
space group	$P2_1/n$	$P2_1/c$
Z	4	4
ρ_{calcd} (g/cm^3)	2.22	2.05
μ(Mo Kα) (mm^{-1})	2.550	2.278
temp (K)	190	190
$2\theta_{max}$ (deg)	56.6	52.92
no. of obsd reflns ($I > 2\sigma(I)$)	7863	8468
no. of params	460	595
GOF[a]	1.005	0.943
max shift in cycle	0.001	0.002
residuals: R1, wR2[a]	0.0255, 0.0520	0.0303, 0.0700
abs correctn, max/min	SADABS, 0.90/0.67	SADABS, 0.75/0.64
largest peak in final diff map (e$^-$/Å^3)	0.726	1.725

[a] $R1 = \sum_{hkl}(||F_o| - |F_c||)/\sum_{hkl}|F_{obs}|$; $wR2 = [\sum_{hkl}w(|F_o| - |F_c|)^2/\sum_{hkl}wF_o^2]^{1/2}$, $w = 1/\sigma^2(F_o)$; $GOF = [\sum_{hkl}w(|F_o| - |F_c|)^2/(n_{data} - n_{vari})]^{1/2}$.

Results

The new mixed-metal cluster **2** was obtained in 52% yield from the reaction of **1** with $Pt(PBu^t_3)_2$ at 25 °C.[18] The compound crystallizes in three different crystal modifications depending on the crystallization solvent that is used. The crystal structure analyses reveal two isomeric forms for the molecular structure of **2**. One isomer, **2A**, was found in both the triclinic form and one of the monoclinic forms obtained by crystallization from solutions in benzene/octane solvent mixtures at −5 °C. The molecular structure is similar in both of these crystal forms, and the molecule consists of a square pyramidal cluster of five ruthenium atoms with one platinum atom spanning the square base. An ORTEP diagram of the molecule as found in the triclinic form is shown in Figure 1. Selected bond distances and angles of both crystalline forms are listed in Table 3. There is significant bonding to each of the four nearest neighbor ruthenium atoms. The Pt−Ru distances range from 2.7966(5) to 3.1483(6) Å. A carbido ligand lies in the center of the $PtRu_5$ octahedron. A

(20) *SAINT+ Version 6.02a*; Bruker Analytical X-ray System, Inc.: Madison, WI, 1998.
(21) Sheldrick, G. M. *SHELXTL Version 5.1*; Bruker Analytical X-ray Systems, Inc.: Madison, WI, 1997.

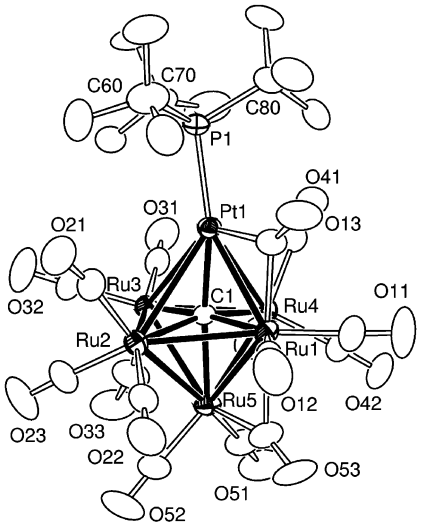

Figure 1. An ORTEP diagram of the molecular structure of **2** as found in the triclinic crystal form **2A** showing 40% thermal ellipsoids.

Table 3. Selected Intramolecular Distances and Angles for **2**, Isomer **2A**[a]

atom	atom	triclinic form distance (Å)	monoclinic form distance (Å)
Pt(1)	P(1)	2.3547(17)	2.361(2)
Ru(1)	Pt(1)	2.7966(5)	2.8133(7)
Ru(2)	Pt(1)	3.1483(6)	3.2603(8)
Ru(3)	Pt(1)	3.1413(5)	3.1454(9)
Ru(4)	Pt(1)	3.1463(5)	3.0139(8)
Ru(1)	Ru(2)	2.9280(7)	2.9186(10)
Ru(1)	Ru(4)	2.9297(7)	2.9295(9)
Ru(1)	Ru(5)	2.8699(7)	2.8786(10)
Ru(2)	Ru(3)	2.8585(7)	2.8953(10)
Ru(3)	Ru(4)	2.8576(7)	2.8415(10)
Ru(4)	Ru(5)	2.7693(8)	2.8025(10)
Ru(1)	C(1)	2.028(6)	2.024(8)
Ru(2)	C(1)	2.079(5)	2.074(8)
Ru(3)	C(1)	2.022(6)	2.034(8)
Ru(4)	C(1)	2.083(5)	2.093(8)
Ru(5)	C(1)	2.151(6)	2.163(8)
Pt(1)	C(1)	2.002(7)	2.079(8)
O(av)	C(av)	1.13(1)	1.14(1)

atom	atom	atom	triclinic form angle (deg)	monoclinic form angle (deg)
P(1)	Pt(1)	Ru(1)	149.58(5)	149.79(6)
Ru(1)	Pt(1)	Ru(4)	58.720(14)	60.246(19)
P(1)	Pt(1)	Ru(3)	124.75(5)	124.38(6)
Ru(3)	Ru(2)	Ru(1)	88.686(19)	88.32(3)
Ru(5)	Ru(3)	Pt(1)	88.777(17)	89.05(2)
Ru(2)	Ru(5)	Ru(3)	60.542(18)	61.51(2)
Pt(1)	C(1)	Ru(5)	172.5(3)	171.6(4)
Pt(1)	C(1)	Ru(3)	99.9(2)	99.8(3)

[a] Estimated standard deviations in the least significant figure are given in parentheses.

single tri-*tert*-butylphosphine ligand is coordinated to the platinum atom. There is one bridging carbonyl ligand between the platinum atom and one of the ruthenium atoms, Ru(1), and because of this, the Pt−Ru(1) bond distance, 2.7966(5) Å (triclinic) and 2.8133(7) Å (monoclinic), is the shortest of all of the Pt−Ru bond distances.

The second monoclinic form, **2B**, was obtained by crystallization from solutions of the complex in diethyl ether solvent. In this crystalline form there are two completely independent molecules in the asymmetric unit. Both are

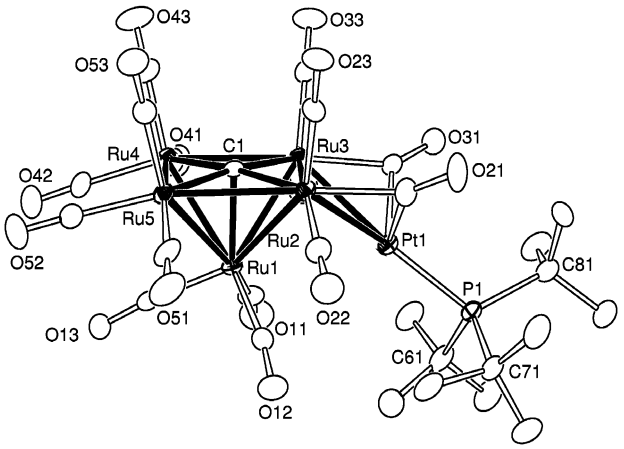

Figure 2. An ORTEP diagram of the molecular structure of **2** as found in the monoclinic crystal form **2B** showing 40% thermal ellipsoids.

Table 4. Selected Intramolecular Distances and Angles for 2 in the Monoclinic Form **2B**[a]

atom	atom	distance (Å)	atom	atom	distance (Å)
Pt(1)	P(1)	2.3307(14)	Ru(4)	Ru(5)	2.8726(6)
Ru(2)	Pt(1)	2.8018(5)	Ru(1)	C(1)	2.119(5)
Ru(3)	Pt(1)	2.7894(5)	Ru(2)	C(1)	2.014(5)
Ru(1)	Ru(2)	2.8829(6)	Ru(3)	C(1)	2.032(5)
Ru(1)	Ru(4)	2.8196(6)	Ru(4)	C(1)	2.030(5)
Ru(1)	Ru(5)	2.8086(6)	Ru(5)	C(1)	2.029(5)
Ru(2)	Ru(3)	2.8928(6)	O(av)	C(av)	1.14(1)
Ru(3)	Ru(4)	2.8407(7)			

atom	atom	atom	angle (deg)	atom	atom	atom	angle (deg)
P(1)	Pt(1)	Ru(2)	147.18(4)	Pt(1)	Ru(2)	Ru(1)	71.146(14)
P(1)	Pt(1)	Ru(3)	150.46(4)	Ru(3)	Ru(1)	Ru(5)	91.253(18)
Pt(1)	Ru(3)	Ru(1)	71.670(14)	Ru(2)	Ru(1)	Ru(4)	90.169(17)

[a] Estimated standard deviations in the least significant figure are given in parentheses.

structurally similar, and a diagram of the molecular structure of one of these molecules is shown in Figure 2. Selected bond distances and angles are listed in Table 4. In this crystalline state the compound has assumed an isomeric structure in which the platinum atom occupies an edge of the square base of the cluster of ruthenium atoms (i.e., the platinum atom is bonded primarily to only two ruthenium atoms; for molecule 1, Pt(1)−Ru(3) = 2.7894(5) Å and Pt(1)−Ru(2) = 2.8018(5) Å; for molecule 2, Pt(11)−Ru(12) = 2.8213(5) Å and Pt(11)−Ru(13) = 2.8282(5) Å). There may also be some weak bonding between the platinum atom and the ruthenium atom at the apex of the Ru_5 square pyramid (Pt(1)−Ru(1) = 3.3076(5) Å and Pt(11)−Ru(11) = 3.1603(5) Å). Two of the carbonyl ligands, C(21)−O(21) and C(31)−O(31), are bridging ligands between the platinum atom and the ruthenium atoms.

The ^{31}P NMR spectrum of **2** in solution at −40 °C shows two phosphorus resonances, δ = 118.2 and 92.7 ppm, both of which exhibit large coupling to platinum (^{195}Pt, 33% natural abundance), indicating that the phosphorus atom is bonded directly to a platinum atom in each case. This indicates that both isomers exist together in equilibrium in solution. The equilibrium is temperature dependent and favors the isomer showing the resonance at δ = 118.2 ppm as the temperature is lowered below −40 °C. For this

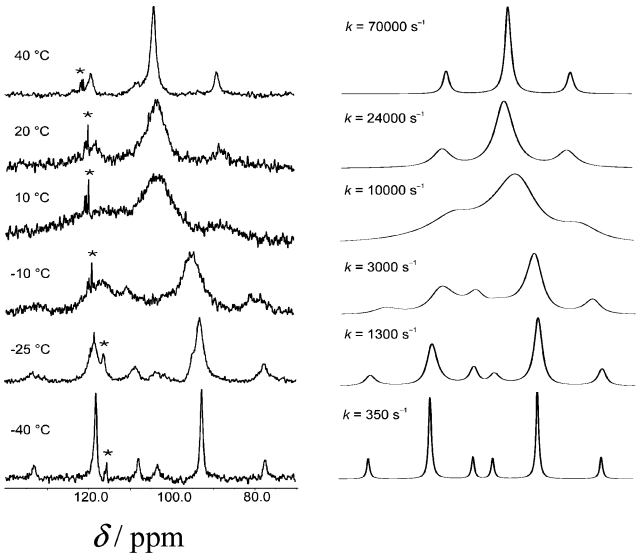

Figure 3. (Left) ^{31}P NMR spectra of compound **2** at various temperatures in toluene-d_8 solvent. Signals labeled with an asterisk are for unidentified impurities. (Right) Computer-simulated spectra at various exchange rates, *k*.

Scheme 1

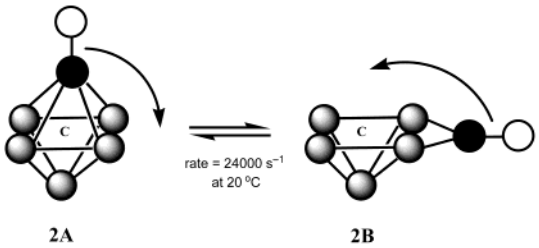

temperature equilibrium the following thermodynamic parameters were determined: $\Delta H° = -1.4(1)$ kcal mol^{-1}, $\Delta S° = -6.1(3)$ cal mol^{-1} K^{-1}. Interestingly, as the temperature is raised above −40 °C, the resonances broaden, coalesce, and average into a single resonance, $\delta = 103.9$ ppm, with appropriate coupling to platinum at 40 °C. These line shape changes confirm that the isomers are interconverting rapidly on the NMR time scale at these higher temperatures. From computer line shape simulations, it was possible to determine the rates of interconversion at the various temperatures and in turn determine the thermodynamic activation parameters: $\Delta G_{298}^{\ddagger} = 11.3(7)$ kcal mol^{-1}, $\Delta H^{\ddagger} = 8.8(5)$ kcal mol^{-1}, $\Delta S^{\ddagger} = -8.4(9)$ cal mol^{-1} K^{-1}; see Figure 3. Notably, no dynamical exchange between the phosphine resonance of the complex and that of free PBu^t_3 was observed at 25 °C when PBu^t_3 was added to the sample.

Our mechanism for interconversion of the two isomers is shown in Scheme 1. This involves a reversible breaking and making of two of the Pt−Ru bonds with a shift of the platinum−phosphine grouping back and forth between the 4-fold Ru_4 site and the 2-fold edge-bridging Ru_2 site, and it occurs at a rate of 24000 per second at 20 °C. The presence of ^{195}Pt−^{31}P coupling in the fast exchange region confirms that there is no Pt−phosphine dissociation in the course of the rearrangement. The absence of exchange between the phosphine ligand in the complex and free phosphine also strongly indicates that the process does not involve dissociation of the entire $PtPBu^t_3$ group because if this happened then one would expect $Pt(PBu^t_3)_2$ to form and the phosphine ligands would be interchanged.

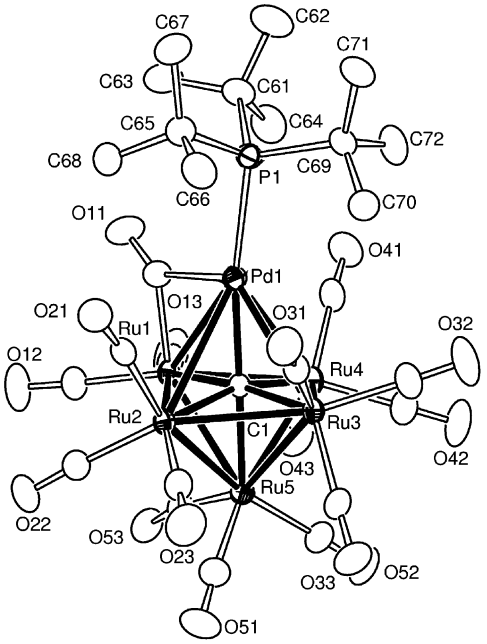

Figure 4. An ORTEP diagram of the molecular structure of **3** showing 40% thermal ellipsoids.

Table 5. Selected Intramolecular Distances and Angles for **3**[a]

atom	atom	distance (Å)	atom	atom	distance (Å)
Pd(1)	P(1)	2.4516(8)	Ru(3)	Ru(4)	2.9142(3)
Ru(1)	Pd(1)	2.7997(3)	Ru(4)	Ru(5)	2.7748(4)
Ru(2)	Pd(1)	3.2666(4)	Ru(1)	C(1)	2.008(3)
Ru(3)	Pd(1)	3.1767(3)	Ru(2)	C(1)	2.070(3)
Ru(4)	Pd(1)	3.0612(3)	Ru(3)	C(1)	2.027(3)
Ru(1)	Ru(2)	2.8927(3)	Ru(4)	C(1)	2.081(3)
Ru(1)	Ru(4)	2.8873(4)	Ru(5)	C(1)	2.171(3)
Ru(1)	Ru(5)	2.9161(4)	Pd(1)	C(1)	2.104(3)
Ru(2)	Ru(3)	2.8364(4)	O(av)	C(av)	1.14(1)

atom	atom	atom	angle (deg)	atom	atom	atom	angle (deg)
P(1)	Pd(1)	Ru(1)	148.91(2)	Ru(5)	Ru(3)	Pd(1)	89.995(8)
Ru(1)	Pd(1)	Ru(4)	58.826(8)	Ru(2)	Ru(5)	Ru(3)	60.644(8)
P(1)	Pd(1)	Ru(3)	126.45(2)	Pd(1)	C(1)	Ru(5)	172.68(13)
Ru(3)	Ru(2)	Ru(1)	89.373(9)	Pd(1)	C(1)	Ru(3)	100.52(10)

[a] Estimated standard deviations in the least significant figure are given in parentheses.

Compound **1** reacts with $Pd(PBu^t_3)_2$ at 25 °C to give two products, **3** in 50% yield and **4** in 6% yield. The yield of compound **4** was increased to 47% when an excess of $Pd(PBu^t_3)_2$ was used in the reaction. Both compounds were characterized by a combination of IR, ^{1}H and ^{31}P NMR, and single-crystal X-ray diffraction analyses. An ORTEP diagram of the molecular structure of **3** is shown in Figure 4. Selected bond distances and angles are listed in Table 5. The structure of **3** is analogous to that of **2A**, consisting of an octahedral cluster of one palladium atom and five ruthenium atoms with an interstitial carbido ligand in the center. The four Pd−Ru distances range from 2.7997(3) to 3.2666(4) Å. The PBu^t_3 ligand is terminally coordinated to the palladium atom, Pd−P = 2.4516(8) Å. There is one bridging carbonyl ligand between the palladium atom and one of the ruthenium atoms,

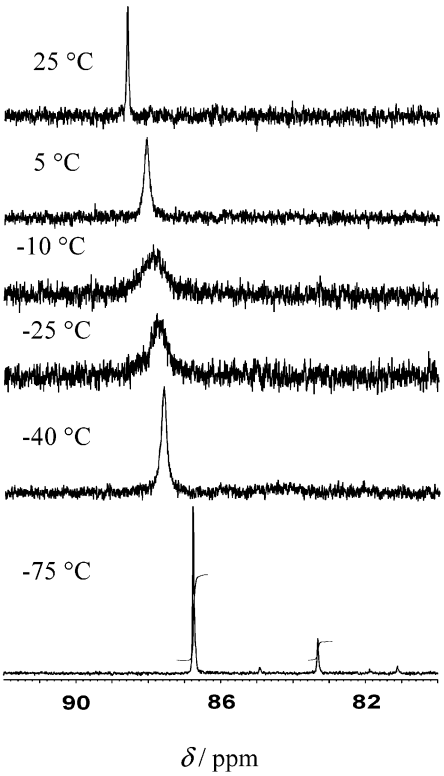

Figure 5. ^{31}P NMR spectra of compound **3** at various temperatures in CD_2Cl_2.

Ru(1), and this is also the shortest Pd−Ru bond, 2.7997(3) Å.

^{31}P NMR spectra of **3** at various temperatures are shown in Figure 5. At −75 °C there are two resonances in a 4:1 ratio in the ^{31}P NMR spectrum. This indicates that **3**, like **2**, is also a mixture of two isomers in a 4:1 ratio in solution at this temperature. ^{31}P NMR spectra of **3** at different temperatures in the range −75 to +25 °C show that both resonances broaden and coalesce (reversibly) as the temperature is raised. The addition of excess free tri-*tert*-butylphosphine at 25 °C showed no exchange with the complex at this temperature. The exchange-broadened spectra were simulated by line shape calculations. These simulations have provided exchange rates and in turn activation parameters for the process, $\Delta G_{298}^{\ddagger} = 10.6(6)$ kcal mol^{-1}, $\Delta H^{\ddagger} = 9.7(3)$ kcal mol^{-1}, and $\Delta S^{\ddagger} = -3(1)$ cal mol^{-1} K^{-1}. The values obtained here are very similar to those obtained for compound **2**, and therefore, a similar mechanism to explain these observations is anticipated; see Scheme 1.

The ^{1}H NMR spectrum of **3** at −90 °C consists of two doublets in a 1:2 ratio. As the temperature is raised the resonances broaden, merge, and appear as a single resonance at 0 °C. These observations are similar to those observed for hindered rotation of the *tert*-butyl group about the P−C bond in tri-*tert*-butylphosphine.[22,23] Accordingly, it is proposed that these spectral changes are due to a similar hindered rotation about the P−C bond in the tri-*tert*-butylphosphine ligand in complex **3**. This process is unrelated to the dynamical interconverion of the two isomers of the cluster. Separate resonances for the major and minor isomers of **3** were not seen at low temperature in the ^{1}H NMR spectra. Presumably, these methyl resonances overlap and are unresolved. Line shape analyses were performed to calculate the exchange rates and in turn the barrier to rotation about the carbon−phosphorus bond. The activation parameters, $\Delta H^{\ddagger} = 8.7(3)$ kcal mol^{-1}, and $\Delta S^{\ddagger} = -7(2)$ cal mol^{-1} K^{-1}, are in good agreement with those observed previously for hindered rotation about the P−C bond in tri-*tert*-butylphosphine, $\Delta H^{\ddagger} = 9.0(4)$ kcal mol^{-1} and $\Delta S^{\ddagger} = 2(4)$ cal mol^{-1} K^{-1}.[23]

(22) Rithner, C. D.; Bushweller, C. H. *J. Am. Chem. Soc.* **1985**, *107*, 7823.
(23) Bushweller, C. H.; Brunelle, J. A. *J. Am. Chem. Soc.* **1973**, *95*, 5949.

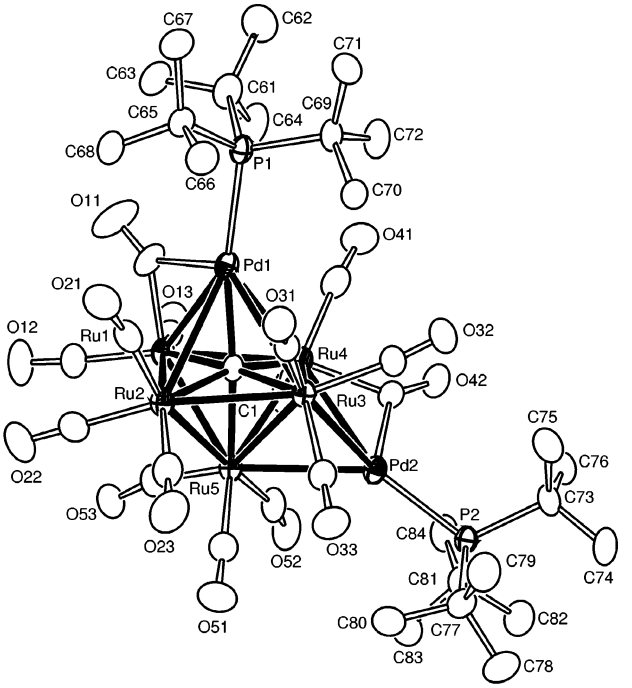

Figure 6. An ORTEP diagram of the molecular structure of **4** showing 40% thermal ellipsoids.

Table 6. Selected Intramolecular Distances and Angles for **4**[a]

atom	atom	distance (Å)	atom	atom	distance (Å)
Pd(1)	P(1)	2.4591(11)	Ru(4)	Ru(5)	2.8058(5)
Pd(2)	P(2)	2.4175(11)	Ru(1)	C(1)	2.016(4)
Ru(1)	Pd(1)	2.7868(5)	Ru(2)	C(1)	2.095(3)
Ru(2)	Pd(1)	3.2195(5)	Ru(3)	C(1)	2.032(4)
Ru(3)	Pd(1)	3.1828(5)	Ru(4)	C(1)	2.073(4)
Ru(4)	Pd(1)	3.1229(5)	Ru(5)	C(1)	2.162(4)
Ru(4)	Pd(2)	2.8694(5)	Pd(1)	C(1)	2.128(4)
Ru(3)	Pd(2)	2.9251(5)	O(av)	C(av)	1.14(1)
Ru(5)	Pd(2)	2.9959(5)			
Ru(1)	Ru(2)	2.9031(5)			
Ru(2)	Ru(3)	2.8364(5)			

atom	atom	atom	angle (deg)	atom	atom	atom	angle (deg)
P(1)	Pd(1)	Ru(1)	146.88(3)	Ru(5)	Ru(3)	Pd(1)	89.013(12)
Ru(1)	Pd(1)	Ru(4)	58.967(11)	Ru(3)	Pd(2)	P(2)	142.43(3)
P(1)	Pd(1)	Ru(3)	128.10(3)	Ru(3)	Pd(2)	Ru(5)	59.019(11)
Ru(3)	Ru(2)	Ru(1)	89.585(12)	Ru(4)	Pd(2)	Ru(3)	60.691(11)

[a] Estimated standard deviations in the least significant figure are given in parentheses.

The molecular structure of **4** is shown in Figure 6. Selected bond distances and angles are listed in Table 6. This compound also consists of an octahedral cluster of one palladium atom and five ruthenium atoms with an interstitial

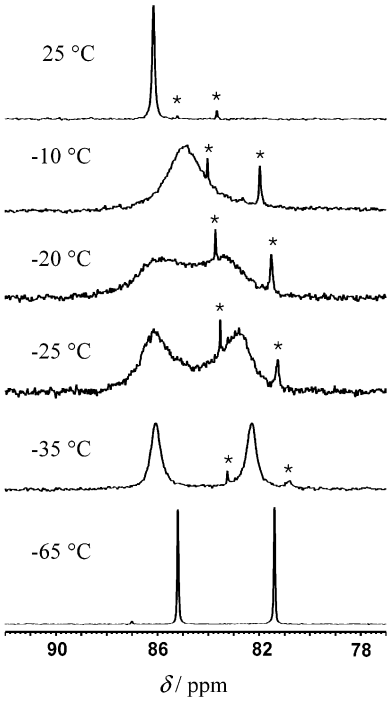

Figure 7. ^{31}P NMR spectra of compound **4** at various temperatures in CD_2Cl_2. Signals labeled with an asterisk are for unidentified impurities.

carbido ligand in the center of the octahedron, but in addition it has a second palladium atom that is capping one of the triangular triruthenium faces of the cluster. Each palladium atom contains one tri-*tert*-butylphosphine ligand. The Pd−P distance for the palladium on the Ru_4 square is slightly longer than the Pd−P distance for the palladium atom on the Ru_3 triangle, 2.4591(11) Å vs 2.4175(11) Å. This is presumably due to steric effects. There are two bridging carbonyl ligands, one between Pd(1) and Ru(1) and the other between Pd(2) and Ru(4). The Pd(1)−Ru and Pd(2)−Ru bond distances lie in the ranges 2.7868(5)−3.2195(5) Å for those on the Ru_4 square and 2.8694(5)−2.9959(5) Å for those on the Ru_3 triangle.

The ^{31}P NMR spectra for the phosphine ligands of **4** at various temperatures are shown in Figure 7. Appropriately, the ^{31}P NMR spectrum of **4** at −65 °C shows two resonances of equal intensity. These resonances are attributed to the two inequivalent phosphine ligands on Pd(1) and Pd(2). Interestingly, the resonances broaden and coalesce (reversibly) as the temperature is raised. The fast exchange limit is reached at 25 °C. Samples containing free *tert*-butylphosphine showed no evidence for dynamical exchange between added free *tert*-butylphosphine and complex **4** at 25 °C. The exchange-broadened spectra were simulated by line shape calculations that have provided exchange rates and in turn activation parameters for the process, $\Delta G_{298}^{\ddagger} = 11(1)$ kcal mol^{-1}, $\Delta H^{\ddagger} = 10.2(4)$ kcal mol^{-1}, $\Delta S^{\ddagger} = -3(2)$ cal mol^{-1} K^{-1}.

A mechanism to explain these observations is shown in Scheme 2. The structure of **4** is represented equally by **4A** and **4B**. In analogy to the dynamics of **2**, it is proposed that the Pd(PBu$^t_3$) group on the square base of the Ru_5 cluster moves to an edge-bridging position en route to a position

Scheme 2

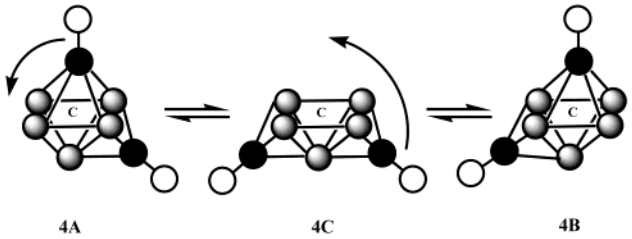

on the Ru_3 triangle that lies opposite the other Pd(PBu$^t_3$) group. This would produce an intermediate, such as **4C**, having two triply bridging Pd(PBu$^t_3$) groups. From **4C** either Pd(PBu$^t_3$) group could shift back to the Ru_4 square to give either **4B**, resulting in interchange of the Pd(PBu$^t_3$) groups, or **4A**, without exchange.

The ^{1}H NMR spectrum for **4** at −90 °C shows four doublets with relative intensities 1:1:2:2. These resonances are attributed to the methyl groups of the inequivalent phosphine ligands. On raising the temperature, these resonances also broaden, coalesce, and then average to a single sharp doublet in the fast exchange limit reached at 25 °C. As with **3**, this is consistent with hindered rotation of the *tert*-butyl groups about the carbon−phosphorus bond in two tri-*tert*-butylphosphine ligands,[22] which are also averaged at the higher temperatures due to the interchange of the palladium atoms between the square and triangle sites of the Ru_5 square pyramid.

Discussion

In previous studies we showed that the compound $PtRu_5(CO)_{15}(PMe_2Ph)(\mu_6\text{-C})$, **5**, exists as a mixture of two octahedral hexanuclear isomers: one having the PMe_2Ph on the platinum atom and another in which the PMe_2Ph is located on one of the ruthenium atoms. The isomers interconvert by a process in which the PMe_2Ph ligand intramolecularly moves back and forth between platinum and ruthenium atoms.[24] However, the activation parameters calculated for this process are much higher ($\Delta H^{\ddagger} = 15.1(3)$ kcal mol^{-1}, $\Delta S^{\ddagger} = -7.7(9)$ cal mol^{-1} K^{-1}) than those observed for **2**. Compound **2** also exists as a mixture of isomers, but in both cases the phosphine ligand is coordinated to the platinum atom. The isomers differ structurally by existing in open and closed cluster forms. Fortunately, we were able to isolate and structurally characterize both forms to prove this. The reason that **2** exists in open and cluster forms may be due to steric destablization of the closed form because of the large size of the tri-*tert*-butylphosphine ligand. Interestingly, the two isomers of **2** interconvert rapidly on the NMR time scale at room temperature. This rate of interconversion is also much faster than the phosphine exchange process that occurs in **5**.

The Pd(PBu$^t_3$) and Pt(PBu$^t_3$) groups are isoelectronic to the Au(PR$_3$)$^+$ group. Skeletal isomerizations of cluster complexes containing Au(PR$_3$)$^+$ have been reported.[15a,25] Recent studies have also shown the pentanuclear metal

(24) Adams, R. D.; Captain, B.; Fu. W.; Pellechia, P. J. *Chem. Commun.* **2000**, 937.

cluster complexes can under go facile rearrangements of their cluster cores.[15a,26] We think that the carbido carbon atom in the interior of the Ru_5 portion of **2**−**4** will prevent similar rearrangements in these compounds.

Metal cluster complexes have frequently been proposed models for metal surfaces albeit they do contain a layer of strongly adsorbed molecules or "ligands" on their surface.[27] The "cluster/surface" analogy was proposed in the late 1970s as a model for understanding some aspects of surface phenomena, especially the nature of small molecule/surface interactions at the atomic level.[28−32] Over the years, however, there have been few good examples of this analogy.[33−35] Here we will make another. One important surface process that has been well studied over the years is known as adatom diffusion.[36−39] The two most important mechanisms are "atom hopping" and "atom exchange".[37−39] In the atom hopping mechanism, an adatom moves on a cubic (100) face from a stable 4-fold site to another by moving over a pair of atoms via an "edge bridge" 2-fold transition state; see the 4-fold, 2-fold, 4-fold example in Figure 8. The interconversion of the two isomers of **2** and **3** could be viewed as one of the elementary steps of this hopping mechanism, in particular the shift of a metal atom from a 4-fold bonding site to a 2-fold site and back.

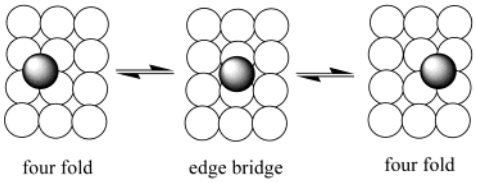

Figure 8. A representation of the adatom hopping mechanism. The shaded surface atom moves from one 4-fold site to another via an edge-bridging, 2-fold transition state.

The ability of a cluster to adopt two different structural arrangements of the metal atoms could also have an important effect on reactivity. For example, in the closed form **2A**, the platinum atom is relatively inaccessible for the addition of a new molecule because it is fully surrounded by ligands and other metal atoms. However, in the open form **2B**, the platinum atom is clearly less sterically encumbered than it is in the closed form. On this basis one would anticipate that reactivity toward ligand additions would be greater in the open form than in the closed form.

Acknowledgment. These studies were supported by the Division of Chemical Sciences of the Office of Basic Energy Sciences of the U.S. Department of Energy under Grant No. DE-FG02-00ER14980 and the USC Nanocenter.

Supporting Information Available: X-ray crystallographic data in CIF format for compounds **2**−**4** and details of the structure solutions and refinement. This material is available free of charge via the Internet at http://pubs.acs.org.

IC020656O

(25) Jungbluth, H.; Stoeckli-Evans, H.; Suss-Fink, G. *J. Organomet. Chem.* **1990**, *391*, 109.
(26) Ohki, Y.; Uejara. N.; Suzuki, H. *Organometallics* **2002**, *21*, 5190.
(27) (a) Raithby, P. R. *Platinum Met. Rev.* **1998**, *42*, 146. (b) Muetterties, E. L. *Bull. Soc. Chim. Belg.* **1976**, *85*, 451. (c) Muetterties, E. L. *Bull. Soc. Chim. Belg.* **1975**, *84*, 959.
(28) Muetterties, E. L. *Chem. Rev.* **1979**, *79*, 93.
(29) Muetterties,E. L. *Chem. Soc. Rev.* **1982**, *11*, 283.
(30) Muetterties, E. L. *Surv. Prog. Chem.* **1983**, *10*, 61.
(31) Albert, M. R.; Yates, J. T., Jr. *The Surface Scientist's Guide to Organometallic Chemistry*; American Chemical Society: Washington, DC, 1987.
(32) Xu, X.; Wang, N.; Zhang, Q. *Bull. Chem. Soc. Jpn.* **1996**, *69*, 529.
(33) Friend,C. M. *Chem. Rev.* **1992**, *92*, 491.
(34) Brait, S.; Deabate, S.; Knox, S. A. R.; Sappa, E. *J. Cluster Sci.* **2001**, *12*, 139.
(35) Brown, D. B.; Johnson, B. F. G.; Martin, C. M.; Wheatley, A. E. H. *J. Chem. Soc., Dalton Trans.* **2000**, 2055.
(36) Tsong, T. T. *Prog. Surf. Sci.* **2001**, *67*, 235.
(37) Kellogg, G. L. *Surf. Sci. Rep.* **1994**, *21*, 1.
(38) Chang, C. M.; Wei, C. M.; Hafner, J. *J. Phys. Condens. Matter* **2001**, *13*, L321.
(39) Zangwill, A. *Physics at Surfaces*; Cambridge University Press: Cambridge, 1988.